Dimerization of a linear Heisenberg chain in the insulating phases of $V_{1-x}Cr_xO_2$

J. P. Pouget and H. Launois
Laboratoire de Physique des Solides, Faculte des Sciences, 91-Orsay, France

T. M. Rice, P. Dernier, and A. Gossard
Bell Laboratories, Murray Hill, New Jersey 07974

G. Villeneuve and P. Hagenmuller
Service de Chimie Minerale Structurale de la Faculte des Sciences de Bordeaux, 33 Talence, France

(Received 25 February 1974)

The nuclear magnetic resonance (NMR) of V^{51} has been studied in the series of compounds $V_{1-x}Cr_xO_2$ between 100 and 350 K. Three insulating phases are clearly distinguished. In the low-temperature M_1 phase only one V site is seen with a positive Knight shift and electric-field gradient identical to the insulating phase of pure VO_2. At temperatures just below the metal-insulator transition a second phase M_2 is stable in which two sites are resolved. One site has a small positive Knight-shift characteristic of a paired V^{4+} site while the other has a negative Knight shift showing a localized V^{4+} site. These two sites are identified as the V atoms on the paired chains and the equispaced chains in $C2/m$ structure of Marezio *et al.* At intermediate temperatures a transitional phase T is stable in which two sites can be resolved by their electric-field gradients. The two sites are progressively differentiated by increasing temperature and Cr concentration and are interpreted as arising from two sets of inequivalent paired chains, one of which is depairing with increasing temperature and Cr concentration. These results are inconsistent with the monoclinic symmetry and a disordered bond model proposed previously for the transitional phase. Triclinic splittings were observed recently by Villeneuve *et al.* and additional crystallographic evidence supporting this result is presented. The magnetic properties are interpreted as a set of noninteracting linear Heisenberg chains and the M_2-T transition as a dimerization of the linear Heisenberg chain. The results demonstrate a breakdown of the band model in the insulating phases.

I. INTRODUCTION

The study of the effects of various dopants on the metal-insulator transitions in the vanadium oxides has in the past been very fruitful.[1-8] In VO_2 it appears that the various dopants fall into two classes. One class is the impurities which enter the insulating phase as 5+ or 6+ ions, e.g. Nb,[5] and give rise to a decrease in the metal-insulator transition temperature at low concentrations but do not stabilize other crystallographic phases. A second class, of which the most studied member is Cr,[3,8] enters as 3+ ions and leads to a complex phase diagram with several new insulating phases, many of whose properties are markedly different from those of the insulating phase of pure VO_2. Since these phases involve large changes in the positions of all of the V atoms and since they are stabilized by concentrations of impurities as low as 0.2 at.% they must be interpreted as alternative phases of pure VO_2 whose free energy is only slightly larger than that of the observed phases of pure VO_2. As the temperature is lowered in the metallic rutile phase (R), for Cr concentrations larger than 0.2 at.%, the metal-insulator transition occurs to a monoclinic phase (M_2) in which the V atoms are split into two sets of chains parallel to the rutile c axis. On one set of chains the V atoms are paired with alternating long and short V-V separations. On the other set of chains, however, the V-V atoms form a zig-zig pattern but remain equally spaced.[8] It has been suggested[8] that these unpaired V atoms are in fact localized V^{4+} ions and we are able to confirm this assignment by the observation of two distinct V^{51} lines in the nuclear-magnetic-resonance (NMR) spectrum. One line has a Knight shift very close to that of pure insulating VO_2 and characteristic of a bonded V-V pair while the other line has a negative Knight shift and a large linewidth as expected for a site with a localized d electron in an insulator. The NMR and the susceptibility data are analyzed in terms of linear Heisenberg chains.

Further lowering of the temperature leads to a transitional insulating phase (T) and finally for concentrations less than 1.5-at.% Cr a transition at still lower temperatures takes place to the monoclinic insulating phase (M_1) of pure VO_2. In the M_1 phase all V atoms are equivalent and paired.

At intermediate temperatures a transitional phase (T) is stable. The properties of the transitional T phase, however, appeared to be inconsistent. A crystallographic refinement[8] gave a monoclinic structure similar to that in M_2 with one half of the V sites paired and one half un-

paired. However, bulk magnetic-susceptibility data showed only a small paramagnetic-susceptibility characteristic of a phase will all V sites paired. A disordered bond model has been put forward by one of us (T.M.R.)[9] which would reconcile the crystallographic and susceptibility data. In this paper we report a detailed study of the NMR of V^{51} in the T phase with varying temperature and concentration of Cr. By measuring the quadrupolar splittings in the NMR spectrum we obtain the electric-field gradient at the V nuclei which is a very sensitive probe of the local environment of the V sites. This enables us to critically test the various models proposed for the T-phase. The data shows clearly that in the T phase the two sublattices of V atoms are progressively differentiated with increasing temperature and Cr concentration with one sublattice remaining totally paired while the other sublattice progressively depairs. Such behavior is inconsistent both with the monoclinic symmetry proposed previously[8] and with the disordered bond model which had been proposed earlier by one of us (T.M.R.).[9]

A careful reexamination of the crystallographic properties was undertaken concurrently with the NMR work.[10] This revealed a small triclinic splitting in the intermediate T phase which is additional evidence favoring our interpretation of the NMR data. Additional crystallographic tests which support the triclinic symmetry are described in Appendix A.

In the model we propose here the nearest neighbor chains to the chains of V atoms which depair are strongly paired and therefore only weakly paramagnetic at all temperatures, and this suggests that we can treat the depairing transition in terms of a dimerization of a set of linear Heisenberg chains which are magnetically uncoupled. There will, however, be some three-dimensional coupling between the chains which are depairing, but this coupling is primarily elastic rather than magnetic.

The interpretation in terms of a dimerized linear Heisenberg chain clearly implies that the $3d$ electrons of V atoms are on the localized side of the Mott transition and that a substantial part of the energy gap in the insulating phase of VO_2 is a correlation Mott-Hubbard gap. In particular the data we report here show an almost continuous transition occurring between the fully paired M_1 phase and the M_2 phase in which one-half of the V sites are localized. This enables us to rule out the recent band scheme proposed by Goodenough and Honig[11] for the M_2 phase.

In Sec. II a description is given of the samples and the experimental apparatus used in the NMR, magnetic-susceptibility, and latent-heat experiments.

The NMR data are presented in Sec. III and the analysis of the NMR spectra to obtain the electric field gradients is described.

In Sec. IV the magnetic susceptibility of a series of samples is given. Latent-heat data at the various transitions is also presented in this section. The discussion of results is continued in Sec. V and the implication for the various models of VO_2 assessed.

II. EXPERIMENTAL

In the absence of single crystals big enough to be studied by NMR methods, the measurements were done on powdered samples. As already discussed by Marezio *et al.*,[8] the exact position of the boundaries in the phase diagram of $V_{1-x}Cr_xO_2$ depends strongly on the preparation and the stoichiometry of the alloys. In this paper we present data collected from powder samples of two different origins.[8,10] The corresponding phase diagrams are presented in Fig. 1. The nominal concentrations, and the transition temperatures determined from x-ray powder patterns are given in Table I. The oxygen stoichiometry of samples A has been checked by thermogravimetric analysis under oxygen atmosphere. Departures from stoichiometry always corresponded to excess of oxygen, giving the formula $V_{1-x}Cr_xO_{2+y}$ with $O < y < 0.005 \pm 0.002$.

The V^{51} NMR measurements were done with cw Varian spectrometers, at frequencies varying from 15 to 22 MHz. Signal averaging was used to observe, when possible, quadrupolar satellites corresponding to the two principal axes for which the values of the electric-field gradients were highest, but was not necessary for the third-axis satellites (smallest field gradients).

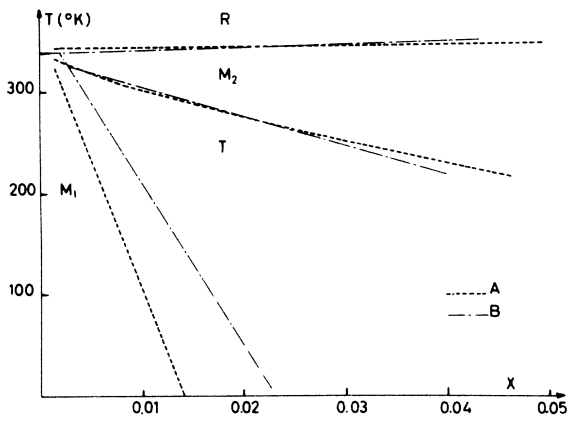

FIG. 1. $V_{1-x}Cr_xO_2$ phase diagrams corresponding to sample preparations A (Ref. 10) and B (Ref. 8).

TABLE I. $V_{1-x}Cr_xO_2$ samples used for the NMR measurements. The two different origins appear in the labels through letters *A* (Ref. 10) and *B* (Ref. 8). The transition temperatures are determined from x-ray powder patterns.

		Transition temperatures		
	x in %	$M_1 \rightarrow T$ (°K)	$T \rightarrow M_2$ (°K)	$M_2 \rightarrow R$ (°K)
A_1	0.3	281	328	343
A_2	0.5	206–235	323	343
A_3	1	unknown (< 77)	305	343
B_1	1	...	...	...

The susceptibility measurements in the temperature range below 300 K were made using a Faraday balance kindly provided by Wohlleben and described elsewhere.[12] The measurements at temperatures above 300 K were carried out also on a Faraday balance by one of us (G.V.) at the University of Bordeaux.

The latent-heat measurements were done on samples A with a differential scanning calorimeter Perkin-Elmer, model DSC2.

III. DATA

The very low symmetry of the nonmetallic phases of $V_{1-x}Cr_xO_2$ yield complicated NMR powder spectra with the $\frac{7}{2}$ nuclear spin of V^{51}. In order to explain how the data were collected and the limits inherent to measurements on powders, we describe first pure VO_2 powder spectra. We will then present the results obtained on a sample with a small Cr concentration which goes through all three phases M_1, M_2, and T. Finally the influence of increasing the Cr concentration will be examined.

A. Pure VO_2

In NMR powder spectra two parts can be distinguished: the central line, due to the $\frac{1}{2} \rightarrow -\frac{1}{2}$ transition, and the quadrupolar spectrum of all the other transitions. (i) For the transition $-\frac{1}{2} \rightarrow +\frac{1}{2}$ first-order quadrupolar effects are not present, and the line shape and position are the result of second-order quadrupolar effects proportional to ν^{-1}, and of an anisotropic Knight shift proportional to ν, where ν is the NMR frequency in constant field (Fig. 2). (ii) The other transitions give rise to line shapes dominated by first-order quadrupolar effects (Fig. 3). A small peak corresponds to the principal axis for which the field gradient is the smallest. Steps correspond to the other principal directions. The distance between $+\frac{3}{2} \rightarrow +\frac{1}{2}$ and $-\frac{1}{2} \rightarrow -\frac{3}{2}$ peaks

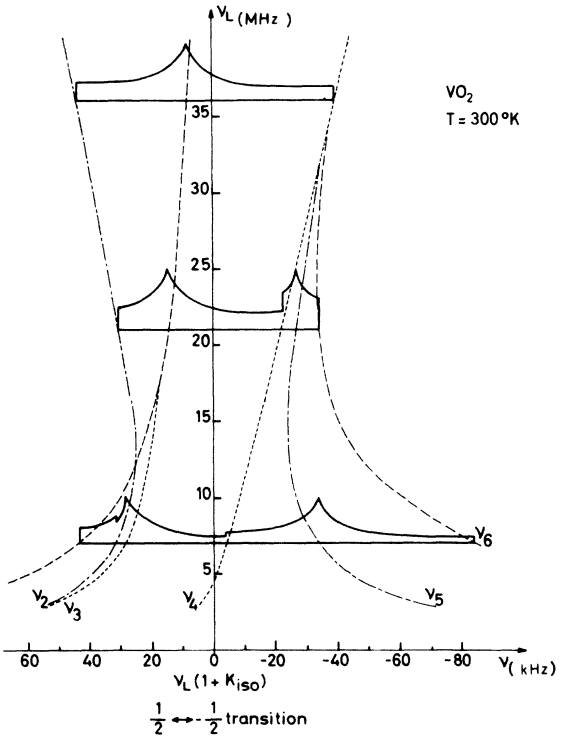

FIG. 2. Powder spectrum of the $-\frac{1}{2} \rightarrow +\frac{1}{2}$ transition in monoclinic VO_2. Typical line shapes are presented for frequencies of 7, 21, and 36 MHz. Dipolar broadening has been neglected. For NMR frequencies $\nu \leq 8.4$ MHz the line shape is determined by second-order quadrupolar effects, for frequencies $\nu \geq 40.5$ MHz by the anisotropic Knight shift. At frequencies of 15 to 22 MHz, used in the present NMR work, second-order quadrupolar effects are still very important.

or steps is due only to first-order quadrupolar effects, and from these the first-order quadrupolar effects can be determined. They are centered on a position which depends on the Knight shift and the second-order quadrupolar effects for this direction and for these transitions.

From a powder spectrum in the presence of anisotropic field gradients, one can then get the following[13]:

(a) The values of the electric-field gradient and Knight shift in the direction of the field-gradient prinicipal axis, when the quadrupolar satellites are observable.

(b) A rough estimate of the isotropic value of the Knight shift, given by the center of gravity of the central line. An exact estimate would require a knowledge of the second-order quadrupolar-effect corrections.

(c) The number of sites contributing to the NMR lines, given by the intensity of the central transition. As can be seen in Fig. 3, a small part of the very broad quadrupolar spectrum will con-

tribute to the NMR central line, and give a systematic error, which is bigger when the field gradients are smaller.

In the monoclinic phase M_1 of pure VO_2 it was possible to observe all the peaks of the quadrupolar spectrum, and steps corresponding to the $+\frac{3}{2} \rightarrow +\frac{1}{2}$ and $-\frac{1}{2} \rightarrow -\frac{3}{2}$ transition. The following experimental values were obtained:

$$V_{yy} = 125 \pm 1 \text{ kHz}, \quad K_y = (0.26 \pm 0.02)\%;$$

$$V_{xx} = 368 \pm 2 \text{ kHz}, \quad K_x = (0.37 \pm 0.02)\%;$$

$$V_{zz} = 490 \pm 3 \text{ kHz}, \quad K_z = (0.15 \pm 0.02)\%;$$

giving a quadrupolar frequency $\nu_Q = 490$ kHz and an anisotropy parameter $\eta = 0.49$. These results are in excellent agreement with the values obtained by Umeda *et al.*[14] on VO_2 single crystals. They determined that the principal axis, i.e., the axis of the smallest principal value of the electric-field gradient, makes an angle of 10° with the rutile c axis (c_R). The other axes lie in a perpendicular plane.

B. $V_{0.997}Cr_{0.003}O_2$

The powder spectrum observed on this sample in the M_1 phase, at temperatures in the range (200–250)°K, is identical to the pure VO_2 spectrum with the same values of the shifts and electrical field gradients and no broadening of the central line nor of the quadrupolar satellites. As one increases the temperature through the $M_1 \rightarrow T$ transition (280°K), no observable change is obtained of the central line, but the quadrupolar spectrum changes. The peaks due to the $+\frac{3}{2} \rightarrow +\frac{1}{2}$ and $-\frac{1}{2} \rightarrow -\frac{3}{2}$ transitions in the y direction (principal axis close to c_R) progressively split, with a total intensity which remains constant. Two types of sites, whose local symmetry is very similar to the M_1 symmetry, are differentiated when temperature increases. The values of the electric-field gradient along the y axis, V_{yy}, are plotted in Fig. 4 versus temperature. For one of the sites (site I) V_{yy} decreases continuously in the T phase. For the second site (site II) V_{yy} increases with increasing temperature. The shape of the central line changes very little with temperature inside the T phase and its intensity remains constant within experimental error (±15%), even at the highest temperatures of the T phase. At these temperatures the $\pm\frac{3}{2} \rightarrow \pm\frac{1}{2}$ (site II) satellites could not be observed because they approach the site-I second satellite in the y direction (transition $\pm\frac{5}{2} \rightarrow \pm\frac{3}{2}$).

A first-order $T \rightarrow M_2$ transition is observed with NMR at 332°K. In the M_2 phase two central lines are obtained. One of them, corresponding to site I, has features very similar to the M_1 and T central lines, except for smaller quadrupolar width. Its intensity is one-half the intensity of the central line in the T phase. The observation of its quadrupolar spectrum gives the following results:

$$V_{yy} = 56 \pm 1 \text{ kHz}, \quad K_y = 0.28 \pm 0.02\%;$$

$$V_{xx} = 293 \pm 2 \text{ kHz}, \quad K_x = 0.36 \pm 0.02\%;$$

$$V_{zz} = 349 \pm 3 \text{ kHz}, \quad K_z = 0.25 \pm 0.02\%.$$

For this site, the y axis is along c_R by symmetry. The electric-field gradient $\nu_Q = 349$ kHz and is smaller than in the M_1 and T phases. The asym-

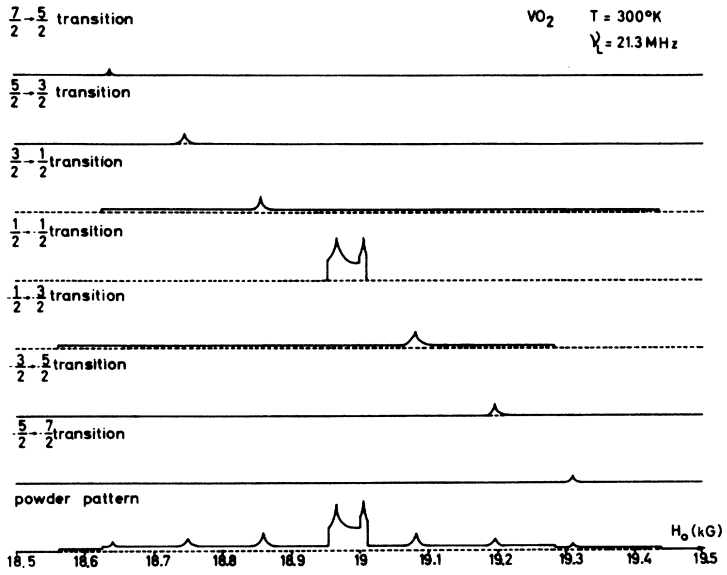

FIG. 3. Schematic powder spectrum of monoclinic VO_2, neglecting the dipolar broadening ($\nu = 21.3$ MHz).

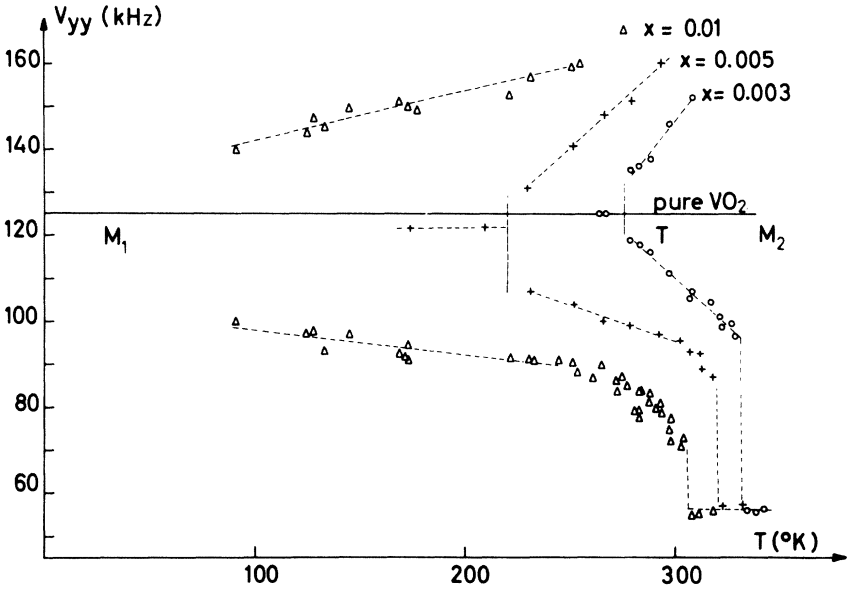

FIG. 4. Smallest value of the electric-field gradient V_{yy} vs temperature in $V_{1-x}Cr_xO_2$. The transition temperatures indicated here by vertical full lines were obtained from x-ray powder pattern. The NMR linewidth prevents a determination of the splitting of the two sites at the lowest temperatures of the T phase, and these results give no information on the order of the $M_1 \rightarrow T$ transition.

metry parameter $\eta = 0.68$. These values are those observed by Umeda *et al.*[15] in a nominally pure VO_2 sample, in a narrow temperature interval near the metal insulator transition. The isotropic shift K_{iso} (= 0.3%) has approximately the same value as in M_1. The second line is shifted negatively, and severely broadened, which makes the observation of the quadrupolar spectrum impossible. The approximate shift obtained from the central line position is $K \approx -0.13\%$ and the linewidth is of the order of 70 G. No changes occur in the spectrum in the small temperature range of the M_2 phase.

At the first-order $M_2 \rightarrow R$ transition (343°K) the two types of sites become equivalent and are both negatively shifted to a position which is very close to that in pure metallic VO_2.

C. Cr concentration dependence

As can be seen from the phase diagram of Fig. 1, increasing Cr concentration stabilizes the T and M_2 phases. The aim of the NMR study of the concentration dependence is to observe the changes on a microscopic scale inside a phase.

No significant change was obtained in the M_1, M_2, and R phases, except some line broadening at low temperatures due to the moments on the Cr site. The results given for $V_{0.997}Cr_{0.003}O_2$ are valid for the highest concentrations.

By contrast, in the T phase, the quadrupolar spectrum and the central line vary with concentration. In Fig. 4 we present the electric-field gradients measured along the smallest-value principal axis y versus temperature for different concentrations. It is clear from this figure that the difference of local symmetry between sites I and II increases with Cr concentration, and that the symmetry of site I at the top of the T phase for the highest concentration is quite near the symmetry it has in the M_2 phase. The shape of the central line is strongly temperature dependent inside the T phase for a Cr concentration of 1% as shown in Fig. 5. First wings develop, and at the highest temperatures of the T phase the central lines of sites I and II are already differentiated. Site I has a relatively narrow central line, unshifted compared to the M_1 line of pure VO_2, while site II has a very broad line, which shifts negatively when the temperature increases. The local symmetry of site I, as well as the magnetic properties of site II observed at the highest temperature in the T phase for $x = 0.01$ are close to those of the M_2 phase. This shows that the transition is less strongly first order for $x = 0.01$ than for lower concentrations.

IV. MAGNETIC SUSCEPTIBILITY AND LATENT-HEAT DATA

The susceptibility as a function of temperature is presented in Fig. 6. The $M_1 \rightarrow T$ phase transition is not observable in the magnetic properties, but the $T \rightarrow M_2$ and $M_2 \rightarrow R$ phase transitions clearly correspond to increases in the susceptibility.

In the M_1 and T phases the susceptibility increases rapidly at low temperature and with the Cr concentration. We define $\Delta\chi$ ($= \chi_{alloy} - \chi_{VO_2}$) as the contribution due to the presence of Cr impurities in these phases. We take $\chi_{VO_2} = 6.5 \times 10^{-5}$ emu/mole.[5] Figure 7(a) shows a plot of $\Delta\chi^{-1}$ versus T for chromium concentrations

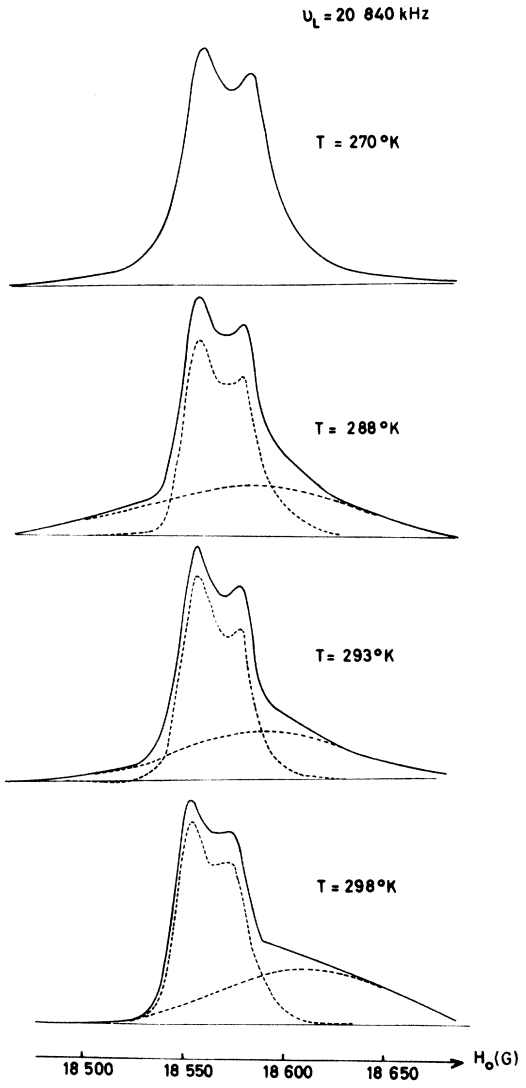

FIG. 5. NMR central line ($-\frac{1}{2} \rightarrow +\frac{1}{2}$ transition) of $V_{0.99}Cr_{0.01}O_2$. The dashed curves represent a decomposition in two lines: one narrow and unshifted due to site I, the other broad and negatively shifted for the highest temperatures of the T phase due to site II.

$x \leq 0.05$. The linearity observed between 10 and 120°K corresponds to Curie-Weiss laws. The Curie constant C increases linearly with x, allowing us to associate with each Cr impurity an effective moment $\mu_{Cr} = (3.76 \pm 0.33)\mu_B$, which is the value obtained for a spin $S = \frac{3}{2}$ with $g = 2$. Deviations occur at temperatures below 10°K as shown in Fig. 7(b) and are not understood.

Approaching the T-M_2 phase transition (Fig. 6) the susceptibility departs from the Curie-Weiss value, and approaches its M_2 value in a continuous way for the high concentrations (5-at.% Cr, 2.5-at.% Cr), but discontinuously for the 1-at.%

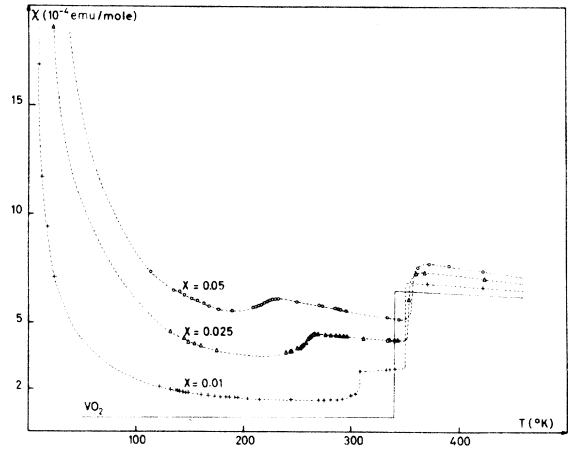

FIG. 6. Magnetic susceptibility of $V_{1-x}Cr_xO_2$ vs temperature.

Cr sample. In this sample the transition T-M_2 looks slightly first order. This transition, as well as the M_2 susceptibility, will be discussed later.

In the rutile metallic phase, the susceptibility and its temperature variation increase with Cr concentration. Since the Knight shift on V sites is independent of Cr concentration the extra magnetization is localized on the Cr sites.

The latent-heat data are summarized in Table II. The value found for pure VO_2 compares very favorably with previous measurements.[16] The $M_2 \rightarrow R$ transition remains strongly first order when the Cr concentration x increases. The $T \rightarrow M_2$ transition corresponds to a much smaller latent heat, and is less strongly first order when x increases. An extrapolation would lead to a $T \rightarrow M_2$ transition without any latent heat for $x \geq 0.035$. The $M_1 \rightarrow T$ transition, showing no observable latent heat, is second order or very slightly first order.

V. DISCUSSION

A. Crystallographic properties

In analyzing the various distortions of the rutile phase which occur in the VO_2 alloys it is convenient to break the rutile phase into two interpenetrating sublattices of V atoms consisting of V chains parallel to the rutile c axis. The two sublattices interact via the oxygens. As pointed out by Marezio *et al.*,[8] if the V atoms pair on one sublattice with alternately long and short V-V distances along the c axis, electrostatic forces cause the V atoms on the second sublattice to move off the c axis toward the oxygen atom whose V neighbors on the first sublattice have

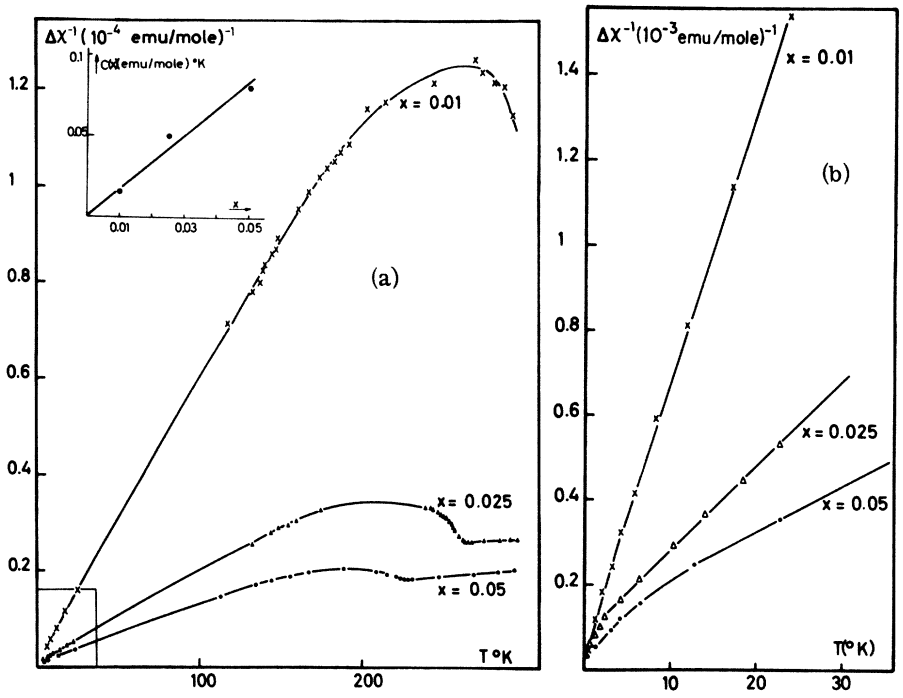

FIG. 7. (a) Inverse of the susceptibility contribution due to the presence of Cr, $\Delta\chi^{-1}$, in the alloys V_{1-x}-Cr_xO_2 vs temperature. The coefficient $C(x)$ of the Curie-Weiss laws obtained at low temperature is plotted vs Cr concentration. (b) Low temperature part of Fig. 7(a).

pulled apart. Thus, the degree of pairing on one sublattice will determine the degree of twisting off the c axis on the second sublattice. In the M_1 phase both sublattices are paired and twisted and are totally equivalent. In the M_2 phase the two sublattices are completely differentiated with one paired but not twisted while the second sublattice is twisted but not paired (see Fig. 8). In the T phase which is the transitional phase between M_1 and M_2, the electric-field gradients show a large variation with temperature and concentration x, as described in Sec. III. In the first place two distinct V sites are always seen in the T phase. If we concentrate on the site-I line which is always unshifted relative to pure VO_2, we notice the variation of the electric-field gradient along a principal axis with temperature in T is monotonic. At low temperatures its value is close to that in M_1 while at higher temperatures

TABLE II. Latent heats in $V_{1-x}Cr_xO_2$.

x	Transitions present for this concentration	Latent heat (cal/mole)
0	$M_1 \rightarrow R$	1030
0.003	$M_1 \rightarrow T$	unmeasurable
	$T \rightarrow M_2$	164
	$M_2 \rightarrow R$	800
0.03	$T \rightarrow M_2$	27
	$M_2 \rightarrow R$	770

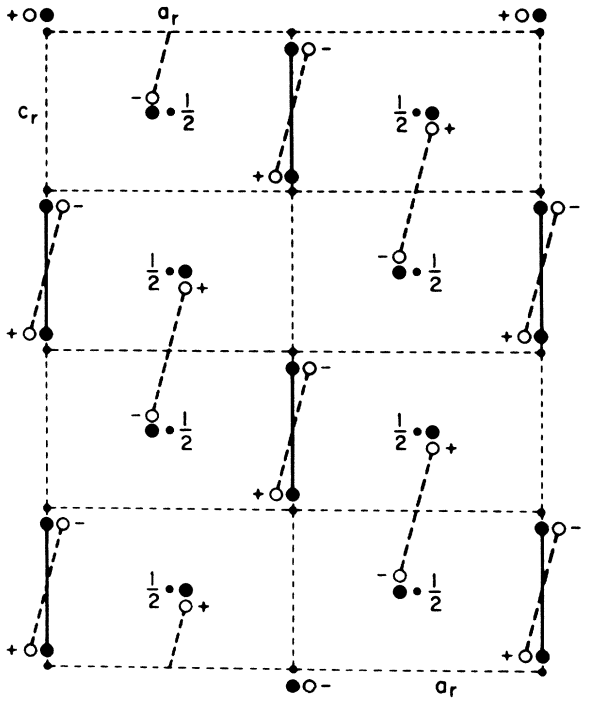

FIG. 8. Comparison of V-V pairing in the three phases (R, M_1, and M_2). In M_1 (open circles) all the vanadium atoms both pair and twist from the rutile positions. In M_2 (filled circles) half of the vanadium atoms pair but do not twist and the other half form unpaired zigzag chains. (The distortions are exaggerated by a factor of 2 for clarity.)

it approaches the corresponding value in M_2. This clearly suggests that this V site is varying in a monotonic way with increasing temperature from the paired and twisted configuration in M_1 to the paired but not twisted configuration in M_2. From the behavior of the central line associated with the other V site we also conclude that it varies monotonically in the T phase between the configurations in M_1 and in M_2. The model which we are led to by the NMR data is that the two V sublattices become progressively differentiated with the degree of twisting on the first sublattice and of bonding on the second sublattice decreasing continuously in T with increasing temperature and x.

In the M_2 phase the monoclinic b axis is along the rutile c axis. However, once one allows both sublattices to pair it is no longer possible to have a two-fold axis along the rutile c axis. The NMR data therefore clearly conflict with the assignment of the transitional phase as monoclinic with $C2/m$ symmetry and the monoclinic b axis along the rutile c axis.[8] Equally it is inconsistent with the proposal put forward earlier by one of us (T.M.R.)[9] of a disordered bond model with average $C2/m$ symmetry. In the low-temperature M_1-phase the monoclinic b axis is along a rutile [100] direction and the two-fold symmetry arises because both sublattices are identical and can be rotated into one another. Therefore in the transitional phase, unequal pairing on both sublattices requires triclinic symmetry. The triclinic distortion, however, is subsidiary to the main effect which is the variation in the V-V bond length on one of the sublattices and as a consequence the deviations from monoclinic symmetry may be very small. Villeneuve *et al.*[10] have recently reported small triclinic splittings in the T phase in the powder patterns of a number of samples. Additional crystallographic tests were performed by one of us (P.D.) and are described in the Appendix. Powder spectra and direct measurements of the unit cell angles on a single crystal show evidence favoring triclinic symmetry. Attempts to perform a single-crystal refinement based on the triclinic symmetry, however, were rendered ambiguous by the additional twinning in the triclinic phase. While the over-all reliability factor was improved by assuming $C\bar{1}$ symmetry, relative to monoclinic $C2/m$ symmetry, the twinning problem prevented an accurate determination of the bonding distances on the weakly bonded sublattice and the concomitant twisting on the strongly bonded sublattice. In summary, the NMR data strongly support the assignment of the T phase as triclinic symmetry with two V sublattices, one more strongly bonded than the other, and while there is no unambiguous single-crystal refinement supporting this assignment, there is powder and other data which supports a very slight distortion of the metric symmetry from monoclinic to triclinic. The lower symmetry and the inevitable crystallographic twinning associated with it, account for the anomalously large thermal parameters reported previously in monoclinic refinements of the T phase[8] and there is now no need to invoke, nor any evidence to support, the disordered bond model.[9]

While the electric-field gradients determined by the NMR have a simple qualitative interpretation, a detailed quantitative explanation is lacking. The precise values of the electric gradients at a V site is determined by the competing fields due to the charge of the $3d$ electron on that V atom and the charge residing on the neighboring O and V atoms. In a crystal such as VO_2 which is not completely ionic but partly covalent, it is not possible to make a reliable calculation of the magnitude of the electric-field gradients and in the absence of such calculation one cannot deduce reliably the temperature and concentration dependence of the distortions such as bonding distance on the more weakly bonded chain, in the T phase.

B. Magnetic properties

Pure VO_2 in its insulating phase has a small temperature-independent Van Vleck paramagnetic susceptibility.[5] On addition of Cr it was shown in Sec. IV that the additional magnetic susceptibility obeys a Curie-Weiss law at low temperatures. The magnitude of moment shows that the Cr atoms enter the lattice as Cr^{3+} ions. This is a consequence of the large Hund's-rule coupling in the half-filled t_{2g} shell of Cr^{3+}.

The Curie-Weiss temperatures are found to be very small ($<10°K$). Examining the curves in Fig. 7(a) we see that there are substantial deviations from Curie-Weiss behavior for temperatures $T>100°K$. We decompose the susceptibility in the insulating phase as

$$\chi = \chi_{VO_2} + C(x)/[T+\Theta(x)] + \delta\chi \ .$$

The remaining susceptibility $\delta\chi$ is plotted versus temperature in Fig. 9.

In the region of stability of the M_2 phase we see from Fig. 9, that $\delta\chi$ is substantial ($\approx 2\times 10^{-4}$ emu/mole VO_2) and approximately independent of temperature and concentration x. The negative Knight shift ($K=-0.13\%$) observed by NMR on the vandiums in site II implies that, in the insulating M_2 phase, half the V sites have a localized $3d$ electron. The Knight shift K is composed of

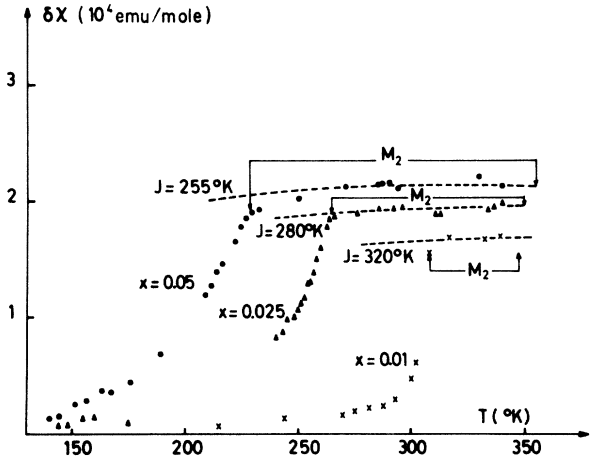

FIG. 9. Remaining susceptibility $\delta\chi\,[=\chi-\chi_{VO_2}-C/(T+\Theta)]$ vs temperature in the T and M_2 phase as a function of temperature for three concentrations. The dashed lines are obtained by fitting the susceptibility to that of a linear Heisenberg chain as calculated by Bonner and Fisher (Ref. 16) using the values shown for the exchange constant J.

a Van Vleck term K_{VV} and of a term due to $3d$ moments K_d. The Van Vleck component K_{VV} is positive and we expect it to lie in the range $0.26\% < K_{VV} < 0.46\%$, determined by the values K_{VV} in the M_1 phase of pure VO_2 and the metallic R phase of pure VO_2 also.[17] The susceptibility due to the localized $3d$ electron can be obtained from K_d, using the hyperfine field of V^{4+} in the R phase of VO_2 ($=-80$ kOe/μ_B),[17] and leads to values for the susceptibility in the range $(1.4-2.1)\times10^{-4}$ emu/mole for $x=0.01$. Comparing to Fig. 9 we see that $\delta\chi$ for this sample has a value, within this range, of $\approx 1.6\times10^{-4}$ emu/mole. This agreement shows conclusively that $\delta\chi$ is arising from the local moments on one-half the V-sites in the M_2 phase. There is uncertainty in the V^{4+} local-moment susceptibility $\delta\chi$ due to possible variation in the Van Vleck susceptibility, which we have taken equal to its value in the M_1 phase of pure VO_2, and due to the possibility of a change of the coupling of the Cr^{3+} to the V^{4+} moments. The first of these possibilities should not be serious since the Van Vleck susceptibility of pure VO_2 is small and insensitive to the M_1-R phase change. The variation of K_{VV} between M_1 and R cited above is mainly due to a change of orbital hyperfine field. However, if there is a strong coupling of the Cr^{3+} and V^{4+} moments this could change the values of $\delta\chi$ substantially for the values of $x=0.025$ and 0.05 but not $x=0.01$. In the last case the Curie-Weiss contribution of the Cr atoms is much smaller than $\delta\chi$. Further $\delta\chi$ is sensitive to the V-V exchange interaction and since the V-V distances do not change appreciably with x there should not be much variation in $\delta\chi$ with x. Therefore, our subtraction procedure seems to be the most reasonable one.

Of the two sublattices of chains parallel to the c axis in M_2, the local moments will be on the V sites which are equispaced along the chains. The magnetic interactions between these chains will be very weak since their nearest-neighbor chains have only bonded V^{4+} sites which are essentially nonmagnetic. We therefore analyze our data using as a model a set of noninteracting linear Heisenberg chains. The magnetic susceptibility of such a chain has been calculated by Bonner and Fisher.[18] In Fig. 9 we show a fit to the values $\delta\chi$ obtained using their results. The magnitude of $\delta\chi$ determines the value of the exchange constant $2J$. We see from Fig. 9 that by adjusting the single parameter J for each value of x we get a good fit to the temperature dependence.

The exchange between the vanadium spins leads to short nuclear relaxation times, and line broadening. In three-dimensional paramagnetic systems the relaxation rates are given[19] by

$$\frac{1}{T_1}=\frac{1}{T_2}=\frac{(2\pi)^{1/2}A^2S(S+1)}{3\hbar^2\omega_{ex}}\ . \qquad (1)$$

Taking $S=\frac{1}{2}$, $\omega_{ex}=5.1\times10^{13}$ sec^{-1} deduced from $J\sim300\,^\circ$K, and the hyperfine constant of V^{4+} in the rutile phase of VO_2 $A/\hbar\approx1.1\times10^9$ sec^{-1}, we obtain a linewidth of 6 G. This value is three times smaller than the experimental value. Such a difference is certainly due to the particularly long-time decay of the spin-spin correlation function in this one-dimensional system. Calculations of this effect exist only in the classical limit of an infinite spin.[20]

Turning our attention to the T phase, we see from Figs. 4 and 9 that the bonding or dimerization transition T-M_2 occurs as a first-order transition for small x and the magnitude of the first-order change decreases with increasing x. For $x\geq0.025$ it appears from the susceptibility that the T-M_2 transition is continuous. The x-ray studies of Villeneuve *et al.*[10] also show a continuous transition in this range and a first-order transition at smaller values of x. While the NMR results do not extend in concentration into the region of the continuous transition they show a consistent variation both in electric-field gradient and in Knight shift of a decreasing first-order change with increasing x (see Figs. 4 and 5). This is confirmed by the latent-heat data discussed above. An extrapolation of the latent-heat results in concentration leads to a transition without any latent heat for $x>0.035$.

The M_2-T transition can be viewed as a bonding

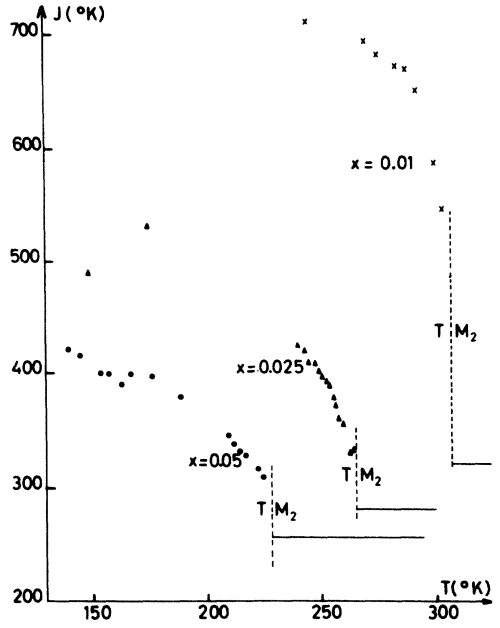

FIG. 10. Exchange constant J obtained using Eq. (2) at each temperature in the T phase plotted vs temperature.

or dimerization transition of a linear Heisenberg chain. From the measurements of the susceptibility $\delta\chi$ it is possible to extract values for the variation of the exchange constant with temperature. At temperatures well below the transition the exchange constant J_1 between the dimerized spins will be much larger than that (J_2) between spins on neighboring dimers and we may treat the dimerized chain as a set of isolated dimers with a simple singlet-triplet spin structure. The singlet-triplet splitting is $2J_1$ and the molar susceptibility from the complex is

$$\chi = \tfrac{1}{4} N \frac{g^2 \mu_B^2}{kT} \frac{S(S+1)}{e^{2J/kT} + 3} , \qquad (2)$$

where N is Avogadro's number. Fitting this result to the values of $\delta\chi$ in Fig. 9 we obtain a series of curves for $J_1(T, x)$ shown in Fig. 10. As the temperature approaches the transition temperature to M_2, J_2 will increase and approach J_1 leading to corrections to the formula (2). Exact numerical calculations for finite alternating Heisenberg chains have been performed by Duffy and Barr.[21] Using their curves it would be possible to incorporate corrections for finite J_2. However, in view of the uncertainties in the procedure in obtaining $\delta\chi$ we have not considered this worthwhile. The corrections are small except when J_2 becomes very close to J_1 and even then the change in susceptibility between the curves with $J_1 = J_2$ and $J_2 = 0$ is not too large for $T \approx J_1$.[21] The curves for $J_1(T)$ in Fig. 10 are approximately quadratic as the temperature approaches the transition temperature indicating that $J_1 - J$ is behaving as an order parameter.

The theory of dimerization of linear magnetic chains has been studied by several authors, using mean-field approximations.[22-24] They find a second-order transition between the dimerized state at low temperatures, and the uniform chain at higher temperatures. Of course in a strictly one-dimensional system fluctuations will prevent an actual phase transition from taking place. In the present case, while the magnetic interactions between V atoms are one-dimensional there are elastic forces that couple the chains in a three-dimensional manner. In such circumstances a mean-field description is applicable. As we remarked earlier the transition observed for $x \lesssim 0.025$ is first order and the magnitude of the first-order transition, as measured microscopically by the V^{51} NMR, decreases with increasing x. The question of why the transition is first order rather than second order as predicted by the simple theories is an open one. The change of symmetry from $C2/m$ in M_2 to $C\bar{1}$ in T halves the number of symmetry transformations and therefore can be second order.[25,26] However, the first-order transition may simply be due to strong-coupling effects in that the exchange interactions are very strongly dependent on distortion. In the strong-coupling limit the Bean-Rodbell theory[27] should be applicable and lead to a first-order transition. Since in the case at hand the transition temperature T-M_2 is almost equal to the exchange constant J in the M_2 phase we are clearly nearer the strong-coupling rather than the weak-coupling limit discussed by Beni and Pincus.[18,19]

When the T-M_2 transition is a large first-order one the magnetic entropy of the T phase is negligible. The magnetic entropy of the M_2 phase can be estimated from the calculations of Bonner and Fisher.[16] For $x = 0.003$ in the region of stability of M_2, $T \approx J$ and from Ref. 16 the entropy S_M per magnetic V site is $S_M \approx 0.4 k_B$. Therefore the latent heat at the T-M_2 transition due to the change in magnetic entropy ΔH_M is

$$\Delta H_M = TS_M = 130 \text{ cal/mole} . \qquad (3)$$

This is comparable to the measured value $\Delta H_{\text{exp}} = 164 \pm 10$ cal/mole. Further, if we assume that the metallic R phase is essentially unchanged by the addition of these small Cr concentrations then we would expect a corresponding reduction in the latent heat at the M_2-R transition when compared to the M_1-R transition in pure VO_2. Experimentally

$$\Delta H_{M_1-R} - \Delta H_{M_2-R} = 230 \pm 40 \text{ cal/mole}, \quad x = 0.003$$
$$= 260 \pm 40 \text{ cal/mole}, \quad x = 0.03 . \tag{4}$$

For the $x = 0.03$ sample, $J = 270°$K and the transition temperature for M_2-R is 340°K leading to a value of $S_M = 0.47$ °K on half the V sites and a value of $\Delta H_M = 160$ cal/mole. If we ascribe the difference to a change in the lattice entropy ΔS_L between M_1 and M_2 then this change

$$\Delta S_L = (\Delta H_{M_1-R} - \Delta H_{M_2-R} - \Delta H_M)/T \tag{5}$$
$$= (0.15 \pm 0.06) k_B \text{ per V} \tag{6}$$

is quite small considering that there is a substantial difference between the distortion in M_1 and M_2. In fact, one might say crudely that M_2 has only half the distortions of M_1 and one is therefore tempted to estimate the change in lattice entropy at M_1-R as twice ΔS_L in Eqs. (5) and (6) leading to an estimate for the lattice latent heat at the M_1-R transition of only 200 cal/mole. This value is close to that obtained by a direct comparison of the entropy of TiO_2 with that of the M_1 phase of VO_2 using experimental heat capacities.[28] However, both these estimates are unreliable since they are based on a comparison between two insulating phases M_1 and M_2 and clearly do not take into account the change in the phonon spectrum caused by the change in electronic character between the insulating M_1 and M_2 phases and the metallic R phase.

As the temperature is lowered in the T phase the two sublattices become more and more similar until at the T-M_1 phase boundary they become identical. This phase transition is governed by the three-dimensional elastic forces and exhibits no measurable latent heat. Again the change of symmetry from $P2/c$ to M_1 to $C\bar{1}$ in T halves the number of symmetry transformations and therefore the transition may be second order.[25,26] The value of J_1, the spin-exchange coupling constant, is not known. In pure VO_2 we may estimate a lower bound on J_1 in M_1 based on the lack of any measurable temperature dependence to the magnitude of the susceptibility. Using Eq. (1) we estimate $2J_1(M_1) \geq 2000°$K.

C. Role of Cr

The main question left unanswered is why does $V_{1-x}Cr_xO_2$ choose to form these curious structures in which an arrangement of equibonded V atoms splits apart in two sublattices, one remaining bonded while the other becomes a set of equidistant V chains in an almost continuous manner. To this question we have no definite answer. Several remarks can be made. In the first place the phase diagram is especially difficult to rationalize if Cr enters the lattice substitutionally since then there should be equal Cr populations on both sublattices. The metal-insulator transition temperature ($\approx 300°$K) is sufficiently low that there can be little migration of the Cr atoms at these temperatures. Without such migration the Cr populations on both sublattices will be equal and there is no driving force which would distinguish the two sublattices.

On the other hand if Cr enters interstitially and the compensating charge to the Cr^{3+} ions is a V^{5+} ion on a nearest-neighbor V site then it is possible that the R-M_2 transition could be driven by an ordering of the V^{5+} ions on one of the sublattices in the M_2 phase. Such an ordering process involves an electron transfer, accompanied by lattice relaxation, and could occur near room temperature. There are, however, other possible

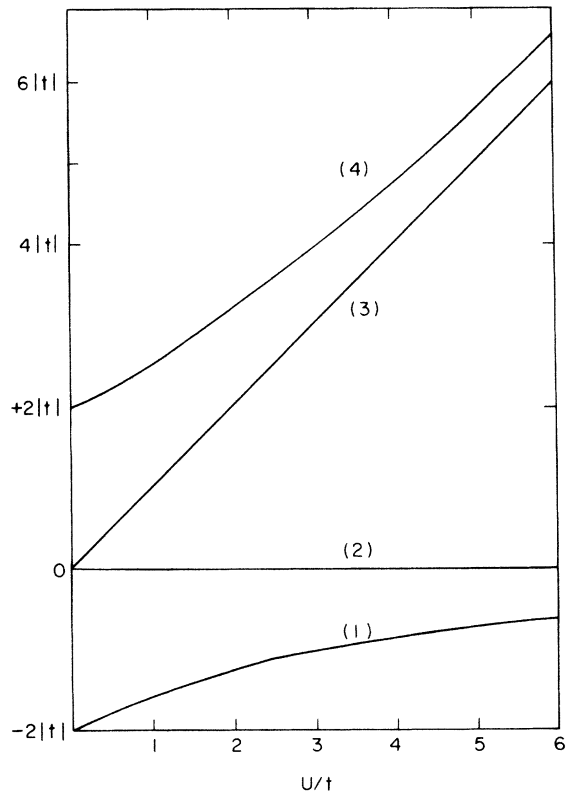

FIG. 11. Energy levels of two electrons in the two-site Hubbard model with hopping parameter t and intra-atomic interaction U. The lowest state (1) is a singlet with energy $E_- = \frac{1}{2}U - (\frac{1}{4}U^2 + 4t^2)^{1/2}$. The level 2 is a triplet with energy $E \equiv 0$. The levels 3 and 4 involve real polar fluctuations with energies $E \equiv U$ and $E_+ = \frac{1}{2}U + (\frac{1}{4}U^2 + 4t^2)^{1/2}$.

TABLE III. Powder pattern of $V_{0.995}Cr_{0.005}O_2$ at 298°K.

hkl ($C2/m$)	hkl ($C\bar{1}$)	d_{obs}	d_{calc} ($C2/m$)	d_{calc} ($C\bar{1}$)	I_{obs}
$\bar{1}11$	$\bar{1}11$	3.298	3.327	3.331	w
	$11\bar{1}$			3.330	
	$1\bar{1}1$			3.302	
$\bar{2}01$	$\bar{2}01$	3.213	3.227	3.230	s
201	201	3.170	3.176	3.176	s
310	$3\bar{1}0$	2.672	2.681	2.684	w
	310			2.681	
220	$2\bar{2}0$	2.422	2.438	2.443	ms
021	220		2.434	2.439	
	$0\bar{2}1$			2.438	
	021			2.437	
$\bar{2}21$	$\bar{2}21$	2.137	2.153	2.157	m, broad
221	221		2.138	2.155	
	$2\bar{2}1$			2.141	
	221			2.138	
$\bar{4}01$	$\bar{4}01$	2.030	2.041	2.042	w
$\bar{2}02$	$\bar{2}02$		2.034	2.036	
401	401	2.011	2.015	2.015	w
202	202		2.009	2.009	
$\bar{3}12$	$\bar{3}12$	1.737	1.739	1.741	w
131	$31\bar{2}$		1.737	1.740	
	$1\bar{3}1$			1.740	
	131			1.739	
510	$5\bar{1}0$	1.731	1.733	1.734	w
	510			1.732	
$\bar{4}21$	$\bar{4}21$	1.658	1.667	1.670	m, broad
$\bar{2}22$	$42\bar{1}$		1.664	1.668	
	$\bar{2}22$			1.665	
	$22\bar{2}$			1.665	
421	$4\bar{2}1$	1.647	1.653	1.655	m, broad
222	421		1.650	1.652	
	$2\bar{2}2$			1.651	
	222			1.649	
$\bar{4}02$	$\bar{4}02$	1.611	1.614	1.615	wm
511	$5\bar{1}1$	1.606	1.609	1.610	wm
	511			1.609	
402	402	1.586	1.588	1.588	wm
331	$3\bar{3}1$	1.524	1.525	1.527	w
	331			1.525	
$\bar{6}01$	$\bar{6}01$	1.437	1.442	1.442	m, broad
$\bar{1}13$	$11\bar{3}$		1.441	1.442	
$\bar{2}03$	$\bar{1}13$		1.436	1.442	
113	$\bar{2}03$		1.435	1.437	
	$1\bar{1}3$			1.435	
	113			1.435	
601	601	1.425	1.428	1.428	w
620	$6\bar{2}0$	1.340	1.341	1.342	wm
	620			1.340	
023	$0\bar{2}3$	1.335	1.335	1.336	s
	023			1.335	
530	$5\bar{3}0$	1.320	1.321	1.323	w
$\bar{3}13$	$\bar{3}13$		1.320	1.321	
$\bar{2}41$	530		1.319	1.321	
	$31\bar{3}$			1.321	
	$\bar{2}41$			1.321	
	$24\bar{1}$			1.320	

TABLE III. *(continued)*

hkl ($C2/m$)	hkl ($C\bar{1}$)	d_{obs}	d_{calc} ($C2/m$)	d_{calc} ($C\bar{1}$)	I_{obs}
241	$2\bar{4}1$	1.313	1.315	1.317	*wm*
332	241		1.314	1.316	
	$3\bar{3}2$			1.315	
	332			1.314	
531	$40\bar{3}$	1.264	1.264	1.265	*w*
403	531		1.264	1.264	
441	$4\bar{4}1$	1.174	1.174	1.176	*vw*, broad
133	$1\bar{3}3$		1.174	1.175	
242	$2\bar{4}2$		1.174	1.175	
	133			1.175	
	441			1.174	
	242			1.173	

defect arrangements at a Cr impurity and without a knowledge of the defect that Cr^{3+} forms, one cannot come to any definite conclusions for the driving mechanism which differentiates between the two sublattices.

D. General conclusions

Many authors[29-33] have interpreted the metal-insulator transition in pure VO_2 (R-M_1) in terms of a band model. In such a model the energy gap in the M_1 phase arises from the bonding-antibonding splitting of the V-V pairs. However, in this paper, the properties of the insulating phases of $V_{1-x}Cr_xO_2$ have been interpreted in terms of a model of localized spins with a Heisenberg exchange coupling between neighbors. In the M_1 phase there is no clear distinction between the two descriptions. This point is illustrated by examining the Hubbard model for an isolated pair of atoms. We take a single nondegenerate orbital on each site with a hopping matrix element t. In the VO_2 problem this corresponds to the assumption that only the $d_{\|}$ band, arising from the t_{2g} orbitals directed along the c axis, is occupied. The energy-level scheme with one electron per atom is shown in Fig. 11. The lowest eigenvalue with energy

$$E_- = \tfrac{1}{2}U - (4t^2 + \tfrac{1}{4}U^2)^{1/2}$$

is a singlet and there is no level crossing as the intra-atomic Coulomb energy U increases. In the band limit ($t \gg U$) the energy gap to the first excited state is $2|t|$ and corresponds to the energy to promote an electron from a bonding to an antibonding orbital. In the localized limit ($t \ll U$) there is a triplet of states with energy $4t^2/U$ above the lowest singlet. These states are the triplet spin states of a pair of Heisenberg exchange coupled spins. The states involving real polar fluctuations are an energy U above. Clearly in this case there is a continuous evolution from the band to the localized limit. The energy gap between the ground state and the lowest state with polar fluctuations is $\frac{1}{2}U + (4t^2 + \frac{1}{4}U^2)^{1/2}$.

If we consider now a crystal with a chain of pairs of atoms coupled by a hopping integral t' then the levels in Fig. 11 are broadened. In the band limit there will continue to be an energy gap $\approx 2|t - t'|$. In the localized limit the triplet states will broaden into a band of spin excitations of width $\sim t'^2/U$ but the gap to polar excitations will be at $U - 2|t'|$. By looking only at the M_1 phase where all V atoms are bonded, one cannot clearly distinguish the values of the ratios t, t', and U. However, in the limit that both t and t' approach a common value t_0 there is a clear distinction. This is the limit of an equispaced chain appropriate to M_2. It is clear from the measurements of a negative Knight shift and an increased susceptibility in M_2 that the V atoms on the equispaced chain have localized $3d$ electrons. Thus we must have $t_0 \ll U$. The almost continuous evolution between M_1 and M_2 suggests that in M_1 we have also $t < U$ though the experiments reported here do not directly measure t. Earlier resistivity measurements did not show any change at M_2-T or T-M_1 transitions. However, the resistivity is probably extrinsic in origin and not a reliable guide to the behavior of the intrinsic energy gap. In this regard it would be of interest to measure the optical gap in the M_2 phase and compare it to the value in the M_1 phase. A more elaborate band model has been put forward by Goodenough and co-workers.[29,11] They proposed that the addition of Cr stabilized the π^* band (composed of the t_{2g} d orbitals which lie in the plane perpendicular to the rutile c axis) at the expense of the $d_{\|}$ band. They argued that while in M_1 the valence band is totally $d_{\|}$, in M_2 the larger unit cell splits both the $d_{\|}$ and π^* bands and the valence band is composed of equal amounts of $d_{\|}$ and π^* bands. However, it is not possible to account for the NMR and magnetic properties of M_2 on the basis of any

band model. Further the continuous transition, at Cr concentrations of a few percent, between the M_1 and M_2 phases rules out any reordering of the bands between these two phases.

The general point of view that in the insulating phases of VO_2 the $3d$ electrons are localized has been put forward earlier[4,5] to account for the general effects of doping. The studies reported here on the $V_{1-x}Cr_xO_2$ system establish definitively the importance of the intra-atomic Coulomb correlations in the insulating phases of VO_2. Similar conclusions in the metallic phase were deduced from the existence of a high-temperature insulating rutile phase for high niobium doping,[5] and from NMR work in pure metallic VO_2.[17]

ACKNOWLEDGMENTS

One of us (H.L.) is very grateful to D. Wohlleben for his hospitality and help with the magnetic susceptibility measurements. We would like to thank J. Friedel for his interest during this work and F. Desnoyer, R. Comes, D. B. McWhan, and M. Marezio for numerous discussions.

APPENDIX

In this section various crystallographic data on sample B are presented on the T phase of Cr-doped VO_2. Tables III–V pertain to power-diffraction data while Table VI is concerned with single-crystal data. This distinction must be made since the single-crystal data can be influenced by twinning, due to the tetragonal pseudosymmetry,[34] whereas the powder data cannot.

Table III lists the observed and calculated interplanar d spacings of $V_{0.995}Cr_{0.005}O_2$ at 298°K. This pattern was obtained from a Norelco camera of 114.6-mm diam and Cr $K\alpha$ (2.2909-Å) radiation. For comparison, the Miller indices hkl are given for both the monoclinic cell $C2/m$ and the triclinic cell $C\bar{1}$ along with the observed intensities and calculated d spacings. The lattice parameters for both cells, determined by least-squares refinement from these data, are reported in Table IV.

TABLE IV. Lattice parameters of $V_{0.995}Cr_{0.005}O_2$ at 298°K.

$C2/m$	$C\bar{1}$
$a = 9.081(1)$	9.084(1)
$b = 5.7806(7)$	5.7906(8)
$c = 4.5162(6)$	4.5182(6)
$\alpha = 90.00$	90.03(1)
$\beta = 90.91(1)$	90.98(1)
$\gamma = 90.00$	90.10(1)

TABLE V. Diffraction data for a resolved set of reflections for $V_{0.99}Cr_{0.01}O_2$ at 298°K.

hkl $(C\bar{1})$	d_{obs}	d_{calc}[a]
$\bar{2}21$	2.158	2.157
$22\bar{1}$	2.152	2.155
$2\bar{2}1$	2.143	2.141
221	2.136	2.138

[a]Based on $V_{0.995}Cr_{0.005}O_2$ least-squares lattice parameters at 298°K.

IV. One can see that either cell fits the data equally well and this ambiguity stems from the fact that a considerable number of reflections were unresolved. However, in confirmation of line splittings originally observed by Villeneuve *et al.*,[10] Table V shows the unique set of reflections $(\bar{2}21, 22\bar{1}, 2\bar{2}1, 221)$ clearly resolved in a $\frac{1}{4}$°/min scan of T phase $V_{0.99}Cr_{0.01}O_2$ by Philips/Norelco diffractometer. From scans of the strongest reflections $(\bar{2}01)$ and (201) it is also evident that at 298°K this material is essentially single phase. That is, one could not have mixtures of phases M_2, T or M_1, T since the former requires extra peaks $(\bar{2}01)$ and (201) with greater 2θ separation than the T peaks while the latter mixture requires an extra single peak where these two reflections have coalesced. None of these extra peaks were observed. Therefore the ambiguity is removed in this example and one must conclude

TABLE VI. Selected structural refinement data of $V_{0.995}Cr_{0.005}O_2$ at 298°K.

Space group	$C2/m$	$C\bar{1}$
Number of observations		
$C2/m$ averaged F_0	392	392
$C\bar{1}$ averaged F_0	645	645
Number of variables	36	58
R factor[a]		
$C2/m$ averaged F_0	0.0268	0.0249
$C\bar{1}$ averaged F_0	0.0303	0.0289
wR factor[b]		
$C2/m$ averaged F_0	0.0377	0.0346
$C\bar{1}$ averaged F_0	0.0392	0.0375
$wR(C2/m)/wR(C\bar{1})$		
$C2/m$ averaged F_0	1.0896	
$C\bar{1}$ averaged F_0	1.0453	
$\mathcal{R}^c_{22,587,0.005} = 1.0366$		

[a]$R = \Sigma|F_0 - F_c|/\Sigma|F_0|$, where F_0 and F_c are the observed and calculated structure factors, respectively.

[b]$wR = [\Sigma w(F_0 - F_c)^2]^{1/2}/[\Sigma(wF_0)^2]^{1/2}$, where $w = 1/0.10 \times F_0$ for all $|F_0| \geq 15$ and $w = 0.667$ for all $|F_0| < 15$.

[c]$\mathcal{R}_{22,587,0.005}$ is the Hamilton $\mathcal{R}$ value at the 0.005 significance level for the hypothesis that $C2/m$ is the correct space group.

from powder data that the symmetry is indeed triclinic.

Single-crystal intensity data were collected semiautomatically at 298°K from a spherically ground crystal of $V_{0.995}Cr_{0.005}O_2$ with a paper-tape controlled GE-XRD5 x-ray diffractometer. The radiation used was Mo $K\alpha$ and the sample was oriented with a^* and b^* in the xy plane leaving c^* nearly coincident with the φ axis of the goniostat. Conversion of intensities to structure factors and refinement techniques were the same as previously reported for $V_{0.976}Cr_{0.024}O_2$.[8] Structural refinements were performed with the $C2/m$ and $C\bar{1}$ symmetries where the observed structure factors were also averaged according to both symmetries. As seen from Table VI the statistical fit was better for $C\bar{1}$ regardless of assumed symmetry in the averaging step. Using the Hamilton-R test,[35] the $C2/m$ model may be rejected at the 0.005 significance level. Nevertheless, due to coincident twinning, the positional and thermal parameters did not vary between the two models to any appreciable extent and the standard deviations remained small and nearly identical. A full discussion of twinning has been reported elsewhere for this and other Cr-doped VO_2 samples.[34] It has been assumed that the effects of noncoincident twinning, approximately 11%, were eliminated by the method of data collection. Unfortunately the structural distortion, namely, the extent of "pairing" and "twisting" along both chains of V ions, was not observed in this experiment since corrections for coincident twinning could not be applied in any meaningful way.

[1]D. B. McWhan, T. M. Rice, and J. P. Remeika, Phys. Rev. Lett. 23, 1384 (1969); and D. B. McWhan and J. P. Remeika, Phys. Rev. B 2, 3734 (1970).

[2]M. Israelsson and L. Kihlborg, Mater. Res. Bull. 5, 19 (1970).

[3]G. Villeneuve, A. Bordet, A. Casalot and P. Hagenmuller, Mater. Res. Bull. 6, 119 (1971).

[4]T. M. Rice, D. B. McWhan, and W. F. Brinkman, in *Proceedings of the Tenth International Conference on the Physics of Semiconductors*, Boston 1970, edited by S. P. Keller, J. C. Hensel and F. Stern (AEC, Washington, D. C. 1971), p. 293.

[5]G. Villeneuve, A. Bordet, A. Casalot, J. P. Pouget, H. Launois, and P. Lederer, J. Phys. Chem. Solids 33, 1953 (1953); and J. P. Pouget, P. Lederer, D. S. Schrieber, H. Launois, D. Wohlleben, A. Casalot, and G. Villeneuve, J. Phys. Chem. Solids 33, 1961 (1972); and P. Lederer, H. Launois, J. P. Pouget, A. Casalot and G. Villeneuve, J. Phys. Chem. Solids 33, 1969 (1972).

[6]T. Hörlin, T. Niklewski, and M. Nygren, Mater. Res. Bull. 7, 12 (1972); and 8, 179 (1973).

[7]D. B. McWhan, J. P. Remeika, J. P. Maita, H. Okinaka, K. Kosuge, and S. Kachi, Phys. Rev. B 7, 326 (1973).

[8]M. Marezio, D. B. McWhan, J. P. Remeika, and P. D. Dernier, Phys. Rev. B 5, 2541 (1972).

[9]T. M. Rice, AIP Conf. Proc. 10, 566 (1972).

[10]G. Villeneuve, M. Drillon, and P. Hagenmuller, Mater. Res. Bull. 8, 1111 (1973).

[11]J. B. Goodenough and H. Y. P. Hong, Phys. Rev. B 8, 1323 (1973).

[12]D. Wohlleben, Ph.D. thesis (University of California, San Diego, 1963) (unpublished).

[13]J. F. Bougher, P. C. Taylor, T. Oja, and P. J. Bray, J. Chem. Phys. 50, 4914 (1969).

[14]J. Umeda, H. Kusumoto, and K. Narita, J. Phys. Soc. Jap. Suppl. 21, 619 (1966).

[15]J. Umeda, S. Ashida, H. Kusumoto, and K. Narita, J. Phys. Soc. Jap. 21, 1461 (1966).

[16]O. A. Cook, J. Am. Chem. Soc. 69, 331 (1947); E. J. Ryder, F. S. L. Hsu, H. J. Guggenheim, J. E. Kunzler (unpublished) quoted by C. N. Berglund and H. J. Guggenheim, Phys. Rev. 185, 1022 (1969). G. V. Chandrashekhar, H. L. C. Barros, J. M. Honig, Mater. Res. Bull. 8, 369 (1973).

[17]J. P. Pouget, Third Cycle Thesis (Orsay, 1972) (unpublished).

[18]J. C. Bonner and M. E. Fisher, Phys. Rev. 135, A640 (1964).

[19]T. Moriya, Progr. Theoret. Phys. 16, 691 (1956).

[20]F. Borsa, D. Hone, C. Scherer, Phys. Rev. B (to be published.

[21]W. Duffy, Jr. and Kevin P. Barr, Phys. Rev. 165, 647 (1968).

[22]G. Beni and P. Pincus, J. Chem. Phys. 57, 3531 (1972).

[23]G. Beni, J. Chem. Phys. 58, 3200 (1973).

[24]J. Y. Dubois and J. P. Carton, J. Phys. (Paris) (to be published).

[25]L. D. Landau and E. M. Lifshitz, *Statistical Physics* (Addison-Wesley, Reading, Mass., 1969), p. 441.

[26]We are grateful to Dr. E. I. Blount for this remark.

[27]C. P. Bean and D. S. Rodbell, Phys. Rev. 126, 104 (1962).

[28]D. B. McWhan (private communication).

[29]J. B. Goodenough, J. Solid State Chem. 5, 145 (1972).

[30]C. N. Berglund and H. J. Guggenheim, Phys. Rev. 185, 1022 (1969).

[31]W. Paul, Mater. Res. Bull. 5, 691 (1970).

[32]C. J. Hearn, J. Phys. C 5, 1317 (1972).

[33]E. Caruthers and L. Kleinman, Phys. Rev. B 7, 3760 (1973).

[34]M. Marezio, P. D. Dernier, and A. Santoro, Acta Crystallogr. A 29, 618 (1973).

[35]W. C. Hamilton, Acta Crystallogr 18, 502 (1965).